

## High dispersed Mo<sub>2</sub>C/AC for gas-phase catalytic direct deoxygenation during lignin pyrolysis

Jiajun Yu,<sup>a</sup> Wujin Xu,<sup>a</sup> Mingxun Zeng,<sup>a</sup> Kai Wu,<sup>a</sup> Wei Jin,<sup>a</sup> Leilei Dai,<sup>a</sup> Shurong Wang<sup>\*b,c</sup> and Huiyan Zhang<sup>\*a</sup>

<sup>a</sup> MOE Key Laboratory of Energy Thermal Conversion and Control, School of Energy and Environment, Southeast University, Nanjing 210096, China

<sup>b</sup> State Key Laboratory of Clean Energy Utilization, Zhejiang University, Hangzhou 310027, China

<sup>c</sup> School of Mechanical and Power Engineering, Shenyang University of Chemical Technology, Shenyang 110142, China

### Supplementary Material

#### *Organic solvent lignin extraction*

Birch lignin, pine lignin, and wheat straw lignin were extracted using an organic solvent method. First, 60 g of raw material with a particle size of 60-200 mesh, 430 mL of 1,4-dioxane, and 50 mL of 2 mol/L HCl solution were added to a 1000 mL round-bottom flask. N<sub>2</sub> gas was introduced to expel air, and the flask was then heated to 110 °C and stirred for 1.5 h. After the reaction, the flask was cooled to room temperature under a N<sub>2</sub> atmosphere. The mixture was filtered to collect a black liquid. The black liquid was further concentrated using a rotary evaporator, after which the concentrated liquid was slowly added to 2 L of water under continuous stirring. The mixture was allowed to stand for 24 h, yielding a yellow precipitate. The precipitate was washed with deionized water until the filtrate became neutral, resulting in crude lignin. The crude lignin was redissolved in 60 mL of an acetone-water solution (acetone: water = 9:1), and the resulting mixture was slowly added to ice water for further purification. After repeated filtration and washing, the solid lignin was

---

collected and dried at 60 °C in a vacuum oven to obtain the respective lignin.

#### *Raw materials*

Absolute ethanol, benzene, toluene, xylene, ethylbenzene, n-propylbenzene, phenol, m-cresol, guaiacol, 2,6-dimethoxyphenol, 4-propylphenol, 4-propylguaiacol, 4-propyl-2,6-dimethoxyphenol, phenyl ether, hydroquinone monobenzyl ether, and 2-phenoxy-1-phenylethanol were purchased from Shanghai Aladdin Biochemical Technology Co., Ltd. ZSM-5 (Si/Al=25) was purchased from Nanhua Catalyst Co., Ltd. Ammonium molybdate tetrahydrate ((NH<sub>4</sub>)<sub>6</sub>Mo<sub>7</sub>O<sub>24</sub>·4H<sub>2</sub>O) was purchased from Shanghai Macklin Biochemical Co., Ltd.

#### *Lignin and catalyst characterization techniques*

Elemental analysis (C, H, N, S) of lignin was quantified using an elemental analyzer (Model Vario EL cube, Elementar Analysensysteme, Germany).

The Lignin alkali metal content was analyzed by inductively coupled plasma atomic emission spectroscopy (ICP-OES) with a Thermo IRIS Intrepid II XSP emission spectrometer after dissolving the catalyst in a HF solution.

X-ray diffraction (XRD) of samples was measured using a Bruker D 8 Advance with a Cu K $\alpha$  (1.54 Å) radiation source and theta-theta diffractometer equipped with a Lynx-eye position sensitive detector. Samples were scanned from 20° to 80° (2 $\theta$ ) at a speed of 5°/min.

X-ray photoelectron spectroscopy (XPS) was collected on scanning X-ray microprobe (PHI 5000 Verasa, ULAC-PHI, Inc.) using Al K $\alpha$  radiation and the C1s peak at 284.8 eV as internal standard.

---

Brunauer-Emmett-Teller (BET) of catalyst was measured using Micrometrics ASAP 2460 (Micromeritics, USA). The test condition is vacuum degassing pretreatment at 300 °C for 6 h. BET, t-plot and BJH methods were used to calculate the specific surface area, pore volume and pore size distribution of the sample.

The analysis of temperature-programmed ammonia desorption (NH<sub>3</sub>-TPD) was conducted on a Micromeritics AutoChem II 2920 (American) instrument to characterize the acidity distribution and strength of Mo<sub>2</sub>C/AC-650 catalyst. The test sample was first heated in a He flow at a ramp rate of 10 °C/min to 300 °C and pretreated at this temperature for 1 h to remove surface moisture. Subsequently, the sample was cooled to 50 °C and exposed to a 10% NH<sub>3</sub>/He flow for 1 h to achieve full ammonia adsorption until saturation. Finally, the temperature was increased from 120 °C to 700 °C at a heating rate of 10 °C/min. The desorption process of NH<sub>3</sub> was monitored using a thermal conductivity detector (TCD), resulting in the NH<sub>3</sub>-TPD profile.

For H<sub>2</sub> temperature-programmed reduction (H<sub>2</sub>-TPR), 50 mg of sample was weighed and heated to 300 °C under Ar atmosphere for dehydration and degassing, and maintained at this temperature for 3 h, then cooled down to room temperature. The gas was then switched to 10% H<sub>2</sub>/Ar. After the TCD baseline stabilized, the temperature was ramped to 700 °C, and the change in H<sub>2</sub> concentration was recorded.

Scanning electron microscopy (SEM) images were observed by field-emission scanning electron microscopy (FE-SEM, FEI Quanta 650). Prior to imaging, the samples were coated with platinum using a vacuum sputter coater to ensure conductivity.

Transmission electron microscopy (TEM) was carried out by a JEM-2100F FETEM equipped

---

with energy dispersive X-ray spectrometer (EDX) analyses at 100 kV, EDX elemental mapping were operated at 200 kV. Verasa, ULAC-PHI, Inc.) using Al K $\alpha$  radiation and the C1s peak at 284.8 eV as internal standard. The sample preparation dispersant was ethanol, sonicated for 3 min, and an ultra-thin carbon film copper mesh was used. In addition, the energy spectrum of C, O and Mo in catalyst was scanned.

Thermogravimetric analysis (TGA) was carried out using a TGA55 instrument on lignin and used catalyst. Lignin samples were heated from room temperature to 800 °C under a N<sub>2</sub> purge at a heating rate of 10 °C/min to investigate their thermal stability, decomposition temperature, and char residue yield. The spent catalyst was placed in a quartz crucible and heated from room temperature to 800 °C at the same rate of 10 °C/min, using an O<sub>2</sub>/N<sub>2</sub> gas mixture (O<sub>2</sub> flow 20 mL/min) as the carrier gas. The mass-versus-temperature curves were recorded to assess catalyst coking.

#### *Details of pyrolysis and catalysis experiments*

In the experiment, the feedstock and gas flow rates were kept constant, and the WHSV was adjusted by varying the catalyst dosage. The catalyst was mixed with inert materials and then filled into the catalyst bed.

The diameter of the main pipe of the reactor used in the reaction is 20 mm, with a wall thickness of less than 2 mm. The lower end of the reactor shrinks, with a diameter of 6 mm and a wall thickness of 1.5 mm. The quality of catalyst used in the reaction is adjusted according to WHSV. In the reaction of guaiacol with WHSV=3 h<sup>-1</sup>, the catalyst dosage is 120 mg. Both N<sub>2</sub> and H<sub>2</sub> used in the experiment are high-purity gases with a purity of 99.99%.

---

*Lignin pyrolysis product analysis*

Qualitative analysis of organic compounds in the liquid products was performed using an Agilent gas chromatography-mass spectrometry (GC-MS, Gas Chromatograph 7890B, Mass Spectrometer 5977B), equipped with an RTX-VMS column (30 m × 0.25 mm × 1.4 μm). A 1 μL sample was injected into the injector with a 10:1 split ratio, and the injector temperature was set to 260 °C. The column oven was programmed for temperature increase: initially at 50 °C for 3 min, then increased to 230 °C at a rate of 5 °C/min, with a 10 min hold at 230 °C. The identified compounds were recognized by matching their mass spectra with a standard spectral library, and the main compounds were confirmed through the injection of standard chemicals. The concentration of target compounds was calculated using standard solutions covering the sample concentration range, and the concentration of trace compounds was quantified using typical compound standard solutions.

The ultraviolet-visible (UV-Vis) of the liquid products were measured using a GENESYS 50 UV-Visible spectrophotometer (Thermo Scientific). The liquid products were dissolved in ethanol, and the absorbance curves were recorded within the wavelength range of 200-800 nm. Prior to measurement, ethanol was scanned at the same wavelengths to establish the baseline for subsequent tests.

The concentrations of gaseous products were determined using a Shimadzu GC-2014 gas chromatograph equipped with both a Flame Ionization Detector (FID) and a Thermal Conductivity Detector (TCD). The FID was equipped with an HP-PLOT/Q column (30 m × 0.32 mm × 20 μm) for the separation of CH<sub>4</sub>, C<sub>2</sub>H<sub>4</sub>, C<sub>2</sub>H<sub>6</sub>, C<sub>3</sub>H<sub>6</sub>, and C<sub>3</sub>H<sub>8</sub>. The TCD utilized a TDX-01 column (2 m × 3 mm) for the separation of CO, CO<sub>2</sub>, and CH<sub>4</sub>. High-purity helium (99.999%) was used as the

---

carrier gas. The oven temperature program was set as follows: hold at 45 °C for 5 min, ramp to 120 °C at 15 °C/min and hold for 8 min, then increase to 180 °C at 30 °C/min and hold for 5 min. Quantification of each gas component was performed using calibration with standard gases of known concentrations.

The definitions for monomer recovery ratio, selectivity, yield, and monomer yield, and monomers selective, are as follows:

$$\text{Conversion (\%)} = 100 - \frac{\text{mole of residual reactants}}{\text{mole of feed reactants}} \times 100 \quad (1)$$

$$\text{Deoxygenation ratio (\%)} = 100 - \frac{\text{moles of O in residual reactants} + \text{moles of O in all products}}{\text{moles of O in feed reactants}} \times 100 \quad (2)$$

$$\text{Selectivity (\%)} = \frac{\text{moles of monomer product } i}{\text{total moles of monomer product}} \times 100 \quad (3)$$

$$\text{Monomers mole yield (mol\%)} = \frac{\text{moles of monomer products} + \text{moles of feed reactants}}{\text{moles of feed reactants}} \times 100 \quad (4)$$

$$\text{Product mole yield (mol\%)} = \frac{\text{total moles of all monomer products}}{\text{moles of feed reactants}} \times 100 \quad (4)$$

$$\text{Monomer yield (wt.\%)} = \frac{\text{quality of monomer product } i}{\text{quality of lignin feed}} \times 100 \quad (6)$$

$$\text{Gas yield (wt.\%)} = \frac{\text{quality of gas product } i}{\text{quality of lignin feed}} \times 100 \quad (7)$$

$$\text{Product yield (wt.\%)} = \frac{\text{quality of product } i}{\text{quality of lignin feed}} \times 100 \quad (8)$$

$$\text{E-factor} = \frac{\text{lignin derived waste} + \text{solvent} + \text{catalysts}}{\text{quality of target products}} \times 100 \quad (9)$$

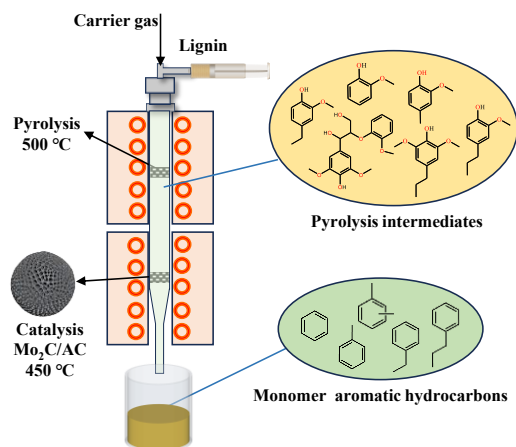


Fig. S1. lignin gas phase pyrolysis and online hydrodeoxygenation reactor and schematic diagram of pyrolysis product evolution.

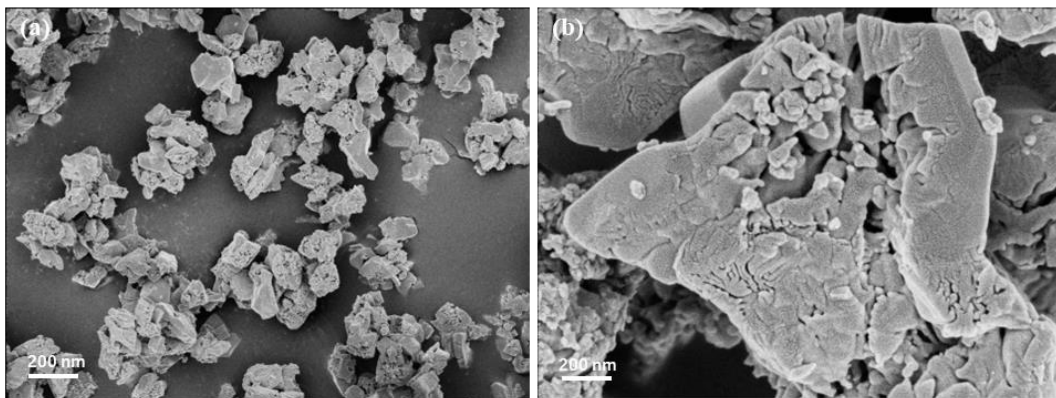


Fig. S2. (a) and (b) SEM image of Mo<sub>2</sub>C/C-650 catalyst.

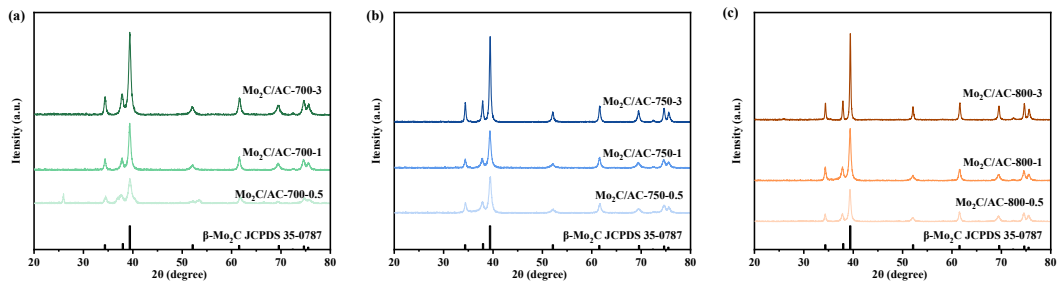


Fig. S3. Variations in the XRD patterns of Mo<sub>2</sub>C/AC catalysts with carburization time: (a) 700 °C; (b) 750 °C; (c) 800 °C.

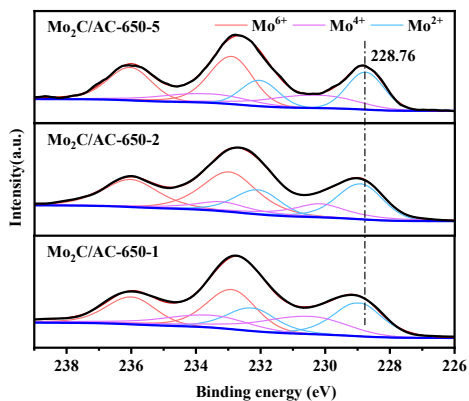


Fig. S4. Variation in the XPS spectra of the Mo<sub>2</sub>C/AC catalyst with carburization time at 650 °C.

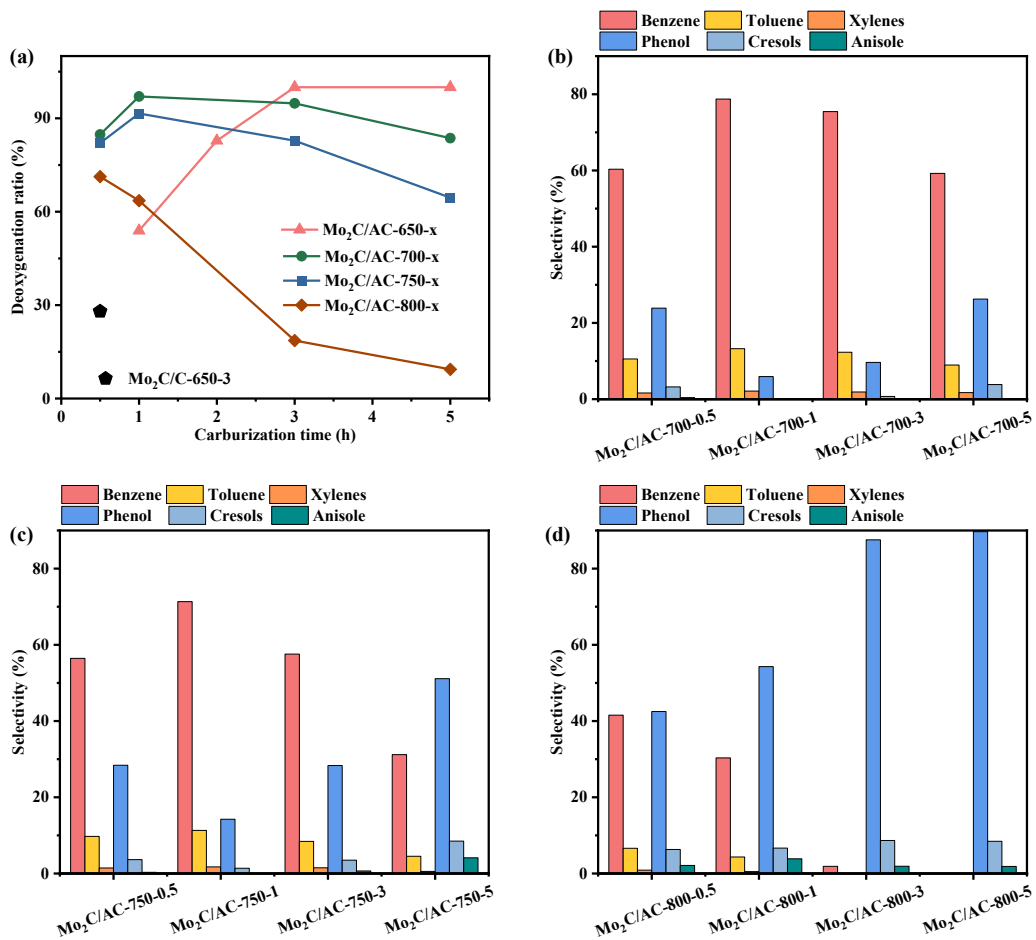


Fig. S5. The influence of changes in carburizing time and carburizing temperature on catalyst performance in the HDO reaction of guaiacol: (a) Changes in guaiacol deoxygenation ratio; (b) The effect of catalyst carburizing time on product distribution at a carburizing temperature of 700 °C; (c) The effect of catalyst carburizing time on product distribution at a carburizing temperature of 750 °C; (d) The effect of catalyst carburizing time on product distribution at a carburizing temperature of 800 °C (WHSV=3 h<sup>-1</sup>, temperature 350 °C, H<sub>2</sub> 1 bar).

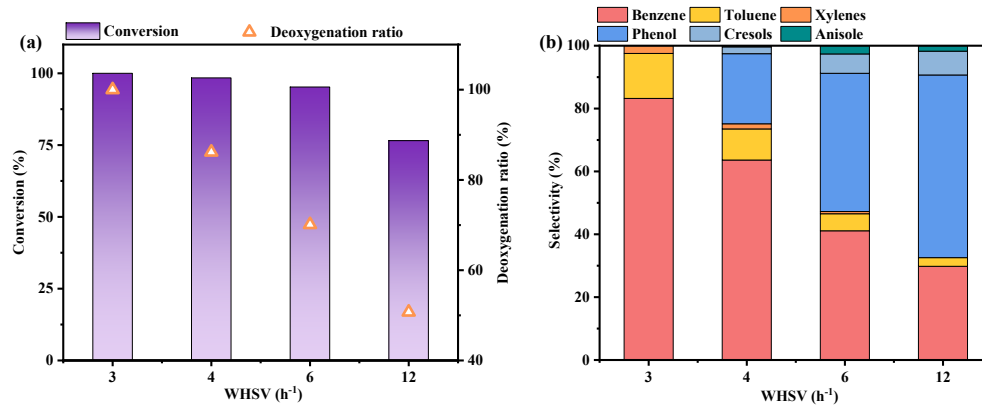


Fig. S6. Conversion of guaiacol HDO at different WHSV: (a) Changes in conversion and deoxygenation ratio; (b) Product distribution changes (Catalyst Mo<sub>2</sub>C/AC-650, temperature 350 °C, H<sub>2</sub> 1 bar).

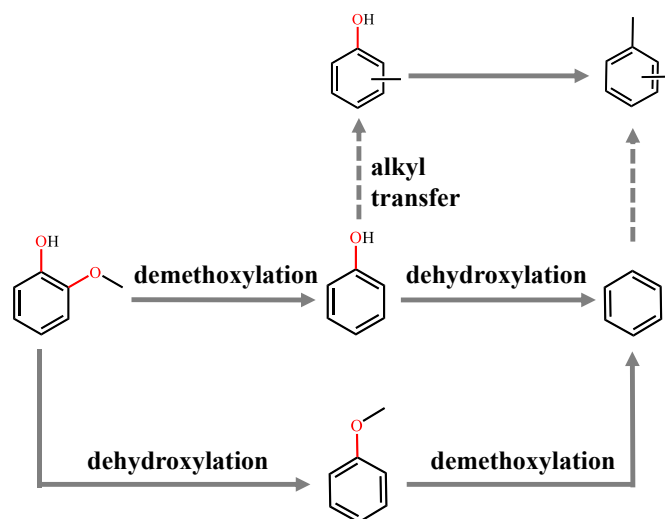


Fig. S7. The evolution of products during the HDO process of guaiacol.

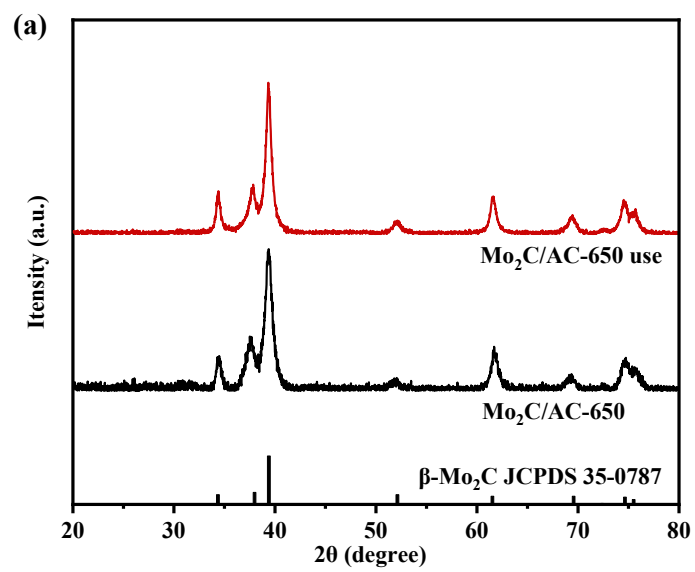


Fig. S8. XRD patterns of Mo<sub>2</sub>C/AC-650 before and after use.

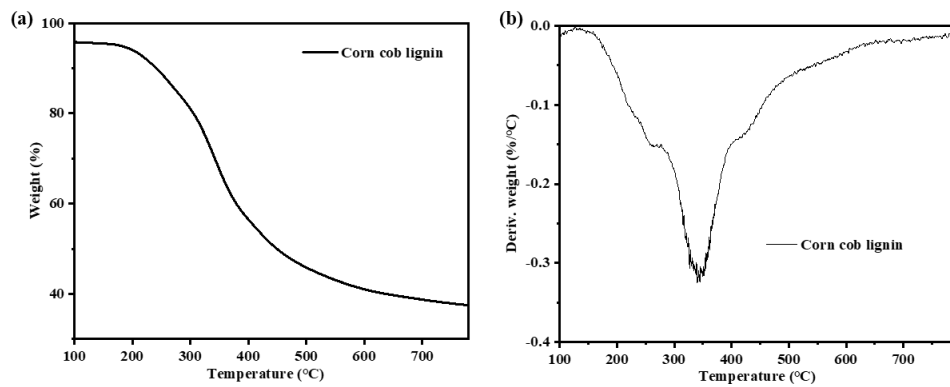


Fig. S9. Thermogravimetric analysis of corn cob lignin: (a) TG curve; (b) DTG curve.

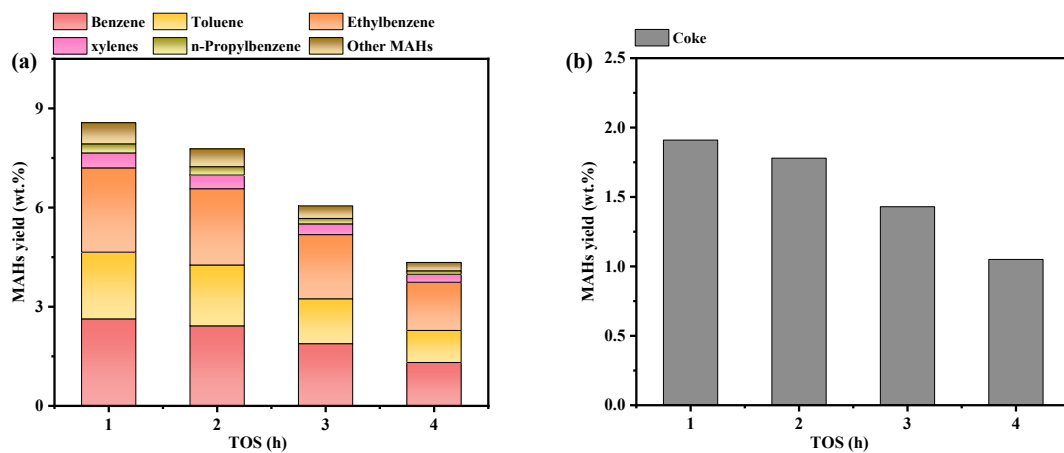


Fig. S10. Long-term stability performance test of Mo<sub>2</sub>C/AC-650 catalyzed HDO of lignin (a) Change in yield of MAHs products; (b) Change in coke. (Catalyst Mo<sub>2</sub>C/AC-650, Catalysis temperature 450 °C, H<sub>2</sub> 1 bar)

Table S1. Proximate analysis of Kraft lignin and corn cob lignin

Raw material	Moisture	Ash	Volatile matter	Fixed carbon
Kraft lignin	1.43	33.51	53.32	11.74
Corn cob lignin	2.8	1.71	59.3	36.19

Table S2. Analysis of alkali metal elements in Kraft lignin

Sample	Metal element content (%)			
	Na	K	Mg	Fe
Kraft Lignin	17.23	1.34	0.11	0.04

Table S3. Element analysis of different types of lignin

Sample	Ultimate analysis (%)				
	C	H	O	N	S
Kraft Lignin	29.90	4.37	45.47	0.87	0.67
Corn cob lignin	62.82	5.51	28.81	1	0.15
Birch lignin	58.82	6.128	34.91	0.14	0
Pine lignin	60.68	6.05	31.82	1.45	0
Wheat straw lignin	62.27	6.8	30.42	0.51	0

Table S4. Crystal structure analysis of catalysts obtained at different carburizing temperatures

Carburization temperature (°C)	Crystal size (nm)	Relative peak area (%)		
		(100)	(002)	(101)
600	5.7±0.4	19.1	29.3	100
650	7.6±0.3	22.5	33.1	100
700	13.2±0.4	20.7	21.3	100
750	22.7±0.2	19.4	19.7	100
800	29.6±0.7	18.2	18.8	100

Carburizing time 3 h.

Table S5. Pore structure of catalysts obtained from different carbon supports

Catalysts	$S_{\text{BET}}$ (m <sup>2</sup> /g)	$S_{\text{micro}}$ (m <sup>2</sup> /g)	$V_{\text{total}}$ (cm <sup>3</sup> /g)	$V_{\text{micro}}$ (cm <sup>3</sup> /g)	Pore diameter (nm) <sup>a</sup>
Lignin carbon	47.2	25.5	0.08	0.04	14.4
Lignin activated carbon	612.7	532.7	0.47	0.27	15.0

a. BJH average pore diameter

Table S6. Comparison of liquid phase products from lignin gas phase catalytic pyrolysis in bench-scale reactors

Entry	Lignin	Catalyst	C/L <sup>a</sup>	Reaction conditions	Monomer yield (wt.%)	Reference
1	Corn cob lignin	Mo <sub>2</sub> C/AC	1	500/450 <sup>b</sup> °C, 1 bar H <sub>2</sub>	8.69 (aromatic hydrocarbons)	This work
2	Birch lignin	Mo <sub>2</sub> C/AC	1	500/450 °C, 1 bar H <sub>2</sub>	11.32 (aromatic hydrocarbons)	This work
3	Organosolv lignin	c-Nb <sub>2</sub> Al <sub>2</sub>	20	700 °C, 1 bar N <sub>2</sub>	2 (aromatic hydrocarbons)	1
4	Organosolv lignin	WO <sub>x</sub> -TiO <sub>2</sub> -Al <sub>2</sub> O <sub>3</sub>	2	650 °C, 1 bar N <sub>2</sub>	1.6 (aromatic hydrocarbons)	2
5	Organosolv lignin	HZSM-5	2	650 °C, 1 bar N <sub>2</sub>	1.9 (aromatic hydrocarbons)	2
6	Acid hydrolysis lignin	Ni/HZSM-5	1:2	45 0 °C, 1 bar N <sub>2</sub>	4.52 (phenols)	3
7	Enzymolysis lignin	NiMo/SiO <sub>2</sub>	-	500/350 °C, 10 bar H <sub>2</sub>	7.01 (57% cycloalkanes, 41% aromatic hydrocarbons)	4
8	Palm shell lignin	Fe/HBeta	1:6	500 °C, 1 bar N <sub>2</sub>	1.72 (aromatic hydrocarbons)	5
9	Palm shell lignin	Fe/HBeta	1:6	500 °C, 1 bar H <sub>2</sub>	5.13 (aromatic hydrocarbons)	5

---



---


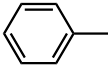
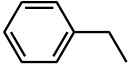
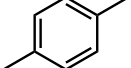
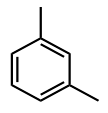
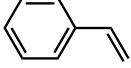
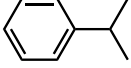
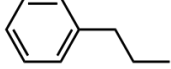
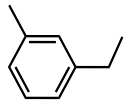
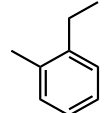
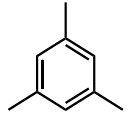
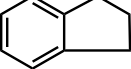
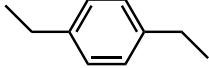
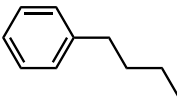
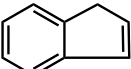
				hydrocarbons)	
10	Enzymatic hydrolysis lignin	HZSM-5 (23)	100 650 °C, 1 bar N <sub>2</sub>	7.49 (aromatic hydrocarbons)	6
11	Organic extracted lignin	HZSM-5 (23)	100 650 °C, 1 bar N <sub>2</sub>	8.36 (aromatic hydrocarbons)	6
12	Klason lignin	HZSM-5 (23)	100 650 °C, 1 bar N <sub>2</sub>	5.91 (aromatic hydrocarbons)	6
13	Alkali lignin	Activated carbon+HZSM-5	3:1 500 °C, 1 bar N <sub>2</sub>	3.0 (aromatic hydrocarbons)	7
14	Poplar organic solvent lignin	HZSM-5	0.6:1 600 °C, 1 bar N <sub>2</sub>	3.17 (aromatic hydrocarbons)	8
15	Wheat straw soda lignin	HZSM-5	0.6:1 600 °C	2.62 (aromatic hydrocarbons)	8

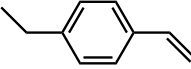
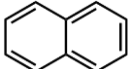
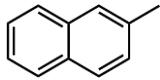
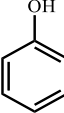
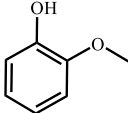
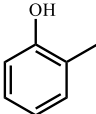
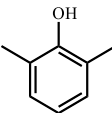
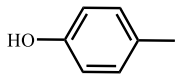
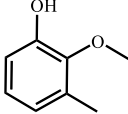
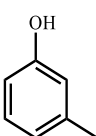
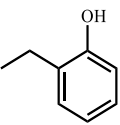
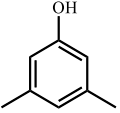
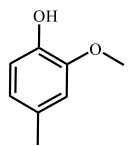
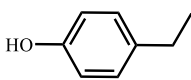
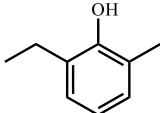
---

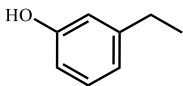
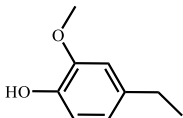
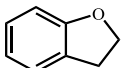
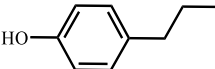
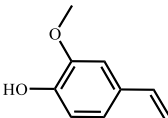
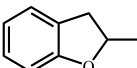
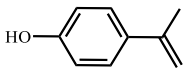
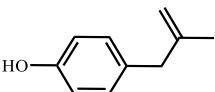
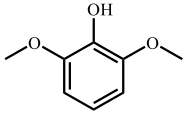
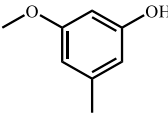
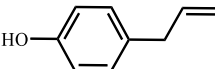
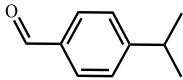
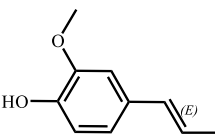
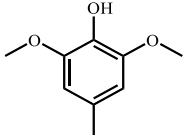
a. Catalyst/lignin feed.

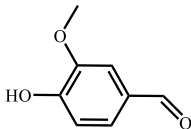
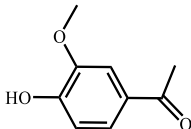
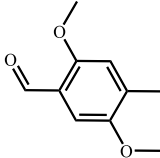
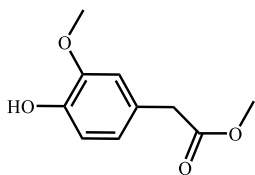
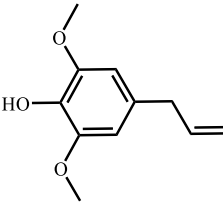
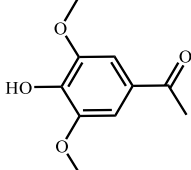
b. 500/450 °C: 500 represents the pyrolysis temperature, 450 represents the catalysis temperature.

Table S7. Distribution of main liquid phase products from gas-phase pyrolysis of corn cob lignin

Entry	Product	Structural formula	Yield (wt.%)	
			No catalyst yield <sup>a</sup>	Mo <sub>2</sub> C/AC-650 catalyst <sup>b</sup>
1	Benzene		0.066	2.532
2	Toluene		0.115	2.171
3	Ethylbenzene		0.037	2.563
4	p-Xylene		0.026	0.342
5	m-Xylene		-	0.143
6	Styrene		-	0.139
7	Benzene, (1-methylethyl)-		-	0.054
8	Benzene, propyl-		-	0.267
9	Benzene, 1-ethyl-3-methyl-		-	0.183
10	Benzene, 1-ethyl-2-methyl-		-	0.063
11	Mesitylene		-	0.014
12	Indane		-	0.076
13	Benzene, 1,4-diethyl-		-	0.016
14	Benzene, n-butyl-		-	0.011
15	Indene		-	0.006

16	Benzene, 1-ethenyl-4-ethyl-		-	0.004
17	Naphthalene		-	0.093
18	Naphthalene, 2-methyl-		-	0.067
19	Phenol		0.448	-
20	Guaiacol		0.153	-
21	Phenol, 2-methyl-		0.147	-
22	Phenol, 2,6-dimethyl-		0.017	-
23	p-Cresol		0.114	-
24	Phenol, 2-methoxy-3-methyl-		0.071	-
25	Phenol, 3-methyl-		0.018	-
26	Phenol, 2-ethyl-		0.013	-
27	Phenol, 3,5-dimethyl-		0.076	-
28	Creosol		0.051	-
29	Phenol, 4-ethyl-		0.324	-
30	Phenol, 2-ethyl-6-methyl-		0.071	-

31	p-Cumenol		0.031	-
32	Phenol, 4-ethyl-2-methoxy-		0.062	-
33	Benzofuran, 2,3-dihydro-		0.364	-
34	Phenol, 4-propyl-		0.023	-
35	2-Methoxy-4-vinylphenol		0.270	-
36	Benzofuran, 2,3-dihydro-2-methyl-		0.055	-
37	Benzene, 1-ethyl-3,5-dimethyl-		0.038	-
38	Phenol, p-(2-methylallyl)-		0.023	-
39	Phenol, 2,6-dimethoxy-		0.060	-
40	3-Methoxy-5-methylphenol		0.021	-
41	Phenol, 4-(2-propenyl)-		0.069	-
42	Benzaldehyde, 4-(1-methylethyl)-		0.008	-
43	trans-Isoeugenol		0.013	-
44	3,5-Dimethoxy-4-hydroxytoluene		0.027	-

45	Vanillin		0.022	-
46	Apocynin		0.006	-
47	4-Methyl-2,5-dimethoxybenzaldehyde		0.013	
48	Benzeneacetic acid, 4-hydroxy-3-methoxy-, methyl ester		0.007	
49	Phenol, 2,6-dimethoxy-4-(2-propenyl)-		0.013	
50	Ethanone, 1-(4-hydroxy-3,5-dimethoxyphenyl)-		0.011	

a. Pyrolysis temperature 500 °C, H<sub>2</sub> 1bar.

b. WHSV=2 h<sup>-1</sup>, Pyrolysis temperature 500 °C, Catalytic temperature 450 °C, H<sub>2</sub> 1bar.

Table S8. The distribution of products from gas-phase pyrolysis of corn cob lignin and online hydrogenation deoxygenation varies with pyrolysis temperature

Pyrolysis temperature (°C)	400	450	500	550	600
Product yield (wt.%)					
MAHs	7.60	7.87	8.59	8.17	7.78
Naphthylenes	0.16	0.21	0.17	0.17	0.22
Unidentified	27.78	24.24	20.99	19.98	23.61
H <sub>2</sub> O	10.40	11.96	13.12	13.67	14.64
Char	37.43	34.95	33.21	30.78	24.87
Coke	1.32	2.12	1.84	1.67	1.54
Gas	15.31	18.65	22.08	25.56	27.34

WHSV=2 h<sup>-1</sup>, Catalytic temperature 450 °C, H<sub>2</sub> 1bar.

Table S9. Comparative analysis of e-factors for different lignin hydrodeoxygenation (HDO) processes

Entry	Catalyst	Conditions	Yield (wt.%)	E-factor	Remarks	Ref.
1	Mo <sub>2</sub> C/AC	500 °C pyrolysis; 450 °C catalysis, 0.1 MPa, continuous operation	8.59-11.32	18.4	Targeted catalysis without the involvement of any solvent	This work
2	HZSM-5	500 °C, 0.1 MPa, continuous operation	2.45	107.9	Low yield of target product, numerous by-products, easy deactivation of the catalyst.	Comparative work
3	HZSM-5	600 °C, 0.1 MPa, continuous operation	5.45	49.3	High reaction temperature, numerous by-products	Comparative work
4	Mo-Co <sub>9</sub> S <sub>8</sub> /Al <sub>2</sub> O <sub>3</sub>	265 °C, 3 MPa, 20 h	14.8	1370.6	Large amount of solvent usage (for heating and separation), low reaction efficiency, batch operation	9
5	Ru/Nb <sub>2</sub> O <sub>5</sub>	250 °C, 0.7 MPa, 6 h	35.5	423.0		10
6	ReS <sub>2</sub> /Al <sub>2</sub> O <sub>3</sub>	600 °C, 3 MPa, 6 h	31	101.94		11

---

**Reference:**

1. D. Yang, J. Huang, Z. Hu, S. Qin, J. Mu, F. Wang, Z. Zhang, Y. Xie, S. Liu and Q. Wang, *Energy*, 2024, 302, 131764, 10.1016/j.energy.2024.131764.
2. C. Wang, J. Ou, T. Zhang, S. Xia, S. Kang, S. Chen, A. Zheng and Z. Zhao, *Fuel*, 2023, 348, 128513, 10.1016/j.fuel.2023.128513.
3. Y. Xu, Z. Fan, X. Li, S. Yang, J. Wang, A. Zheng and R. Shu, *Bioresour. Technol.*, 2024, 399, 130557, 10.1016/j.biortech.2024.130557.
4. T. Li, Y. Meng, L. Yin, B. Sun, W. Zhu, J. Su and K. Wang, *Appl. Catal. B Environ.*, 2024, 353, 124092, 10.1016/j.apcatb.2024.124092.
5. P. S. Rezaei, H. Shafaghat and W. M. A. W. Daud, *Green Chem.*, 2016, 18, 1684-1693, 10.1039/c5gc01935d.
6. H. Yang, K. Norinaga, J. Li, W. Zhu and H. Wang, *Fuel Process. Technol.*, 2018, 181, 207-214, 10.1016/j.fuproc.2018.09.022.
7. H. Zhang, B. Luo, K. Wu, B. Zhao, J. Yu, S. Wang and Y. Tao, *Fuel*, 2022, 318, 123635, 10.1016/j.fuel.2022.123635.
8. J.-Y. Kim, J. H. Lee, J. Park, J. K. Kim, D. An, I. K. Song and J. W. Choi, *J. Anal. Appl. Pyrol.*, 2015, 114, 273-280, 10.1016/j.jaap.2015.06.007.
9. X. Diao, N. Ji, X. Li, Y. Rong, Y. Zhao, X. Lu, C. Song, C. Liu, G. Chen, L. Ma, S. Wang, Q. Liu and C. Li, *Appl. Catal. B Environ.*, 2022, 305, 121067, 10.1016/j.apcatb.2022.121067.
10. Y. Shao, Q. Xia, L. Dong, X. Liu, X. Han, S. F. Parker, Y. Cheng, L. L. Daemen, A. J. Ramirez-Cuesta, S. Yang and Y. Wang, *Nat. Commun.*, 2017, 8, 16104, 10.1038/ncomms16104.
11. P. Sirous-Rezaei, D. Creaser and L. Olsson, *Appl. Catal. B Environ.*, 2021, 297, 120449, 10.1016/j.apcatb.2021.120449.